Antisolvent Crystallization of Anhydrous Sodium Carbonate at Atmospherical Conditions

Harald Oosterhof
Union Minière Research, Kasteelstraat 7, B-2250, Olen, Belgium

Geert-Jan Witkamp and Gerda M. van Rosmalen
Delft University of Technology, Laboratory for Process Equipment, Leeghwaterstraat 44,2628 CA Delft, The Netherlands

When antisolvents are applied to crystallize sodium carbonate from aqueous solutions, the transition temperature at which the hydrates are in equilibrium is decreased. Two models proposed can predict the influence of the amount and type of antisolvent on the transition temperature. Only binary data of the water/sodium carbonate system and measured vapor pressures over ternary soda-saturated mixtures of water and antisolvent are needed. To validate the two models, continuous crystallization experiments were carried out at various temperatures using ethylene glycol (EG) and diethylene glycol (DEG) as antisolvent, in varying concentrations. Both models predict the influence of the antisolvent on the transition temperature with good accuracy. Anhydrous soda with bulk densities of up to 950 kg/m^3 was crystallized at temperatures as low as 80°C.

Introduction

Sodium carbonate can be crystallized as various hydrates. In aqueous solutions, the anhydrous form (Na_2CO_3) is only stable at temperatures above 109°C (Freier, 1978), which is higher than the boiling point of a saturated soda-ash solution (105°C). For producing the desired anhydrous soda from a pure aqueous solution, the boiling temperature needs to be raised above the transition temperature of 109°C by increasing the pressure. Because crystallization in pressured vessels is expensive, the soda is always crystallized at lower temperatures: Na_2CO_3. Monohydrate or $1H_2O$ is then produced, which is subsequently calcined at 150° to 200°C to obtain the anhydrous form. This yields a porous endproduct with a typical bulk density of 550 kg/m^3. A simplified flow sheet of this process is given in Figure 1 (left): a saturated sodium carbonate stream (which is typically encountered in natural soda or "trona" mining, but not in the Solvay process) is taken as the starting point. Energy consumptions of 5.6 MJ/kg sodium carbonate are reported (Weingärtner et al., 1991).

When antisolvent crystallization is used instead of evaporative crystallization, both the high-energy input and the poor crystal quality can be avoided, because the addition of a suitable antisolvent to the mother liquor not only decreases the solubility of the salt but also lowers the water activity. This means that the transition temperature is lowered and anhydrate can be produced directly at lower temperatures, even below the boiling point of the solution (which increases when a high-boiling antisolvent is used). Fleischmann et al. (1984) has observed the same phenomenon in ternary mixtures of water, sodium sulphate, and methanol.

Crystallizing anhydrous sodium carbonate directly allows the calciner to be omitted from the flow sheet, resulting in a considerable saving in energy. In Figure 1, two alternative processes based on the use of nonvolatile (anti)solvents are proposed for the production of anhydrous sodium carbonate at atmospheric pressure.

During evaporative crystallization from mixed solvents (Figure 1, middle), a second solvent (which does not necessarily need to be an *anti*solvent) is added to the crystallizer. A sufficient amount of (anti)solvent lowers the transition temperature, and anhydrous soda will be crystallized at the operating temperature of the crystallizer. The antisolvent preferably has a high boiling point, which means that the boiling point of the solution will be increased, while at the

Correspondence concerning this article should be addressed to H. Oosterhof.

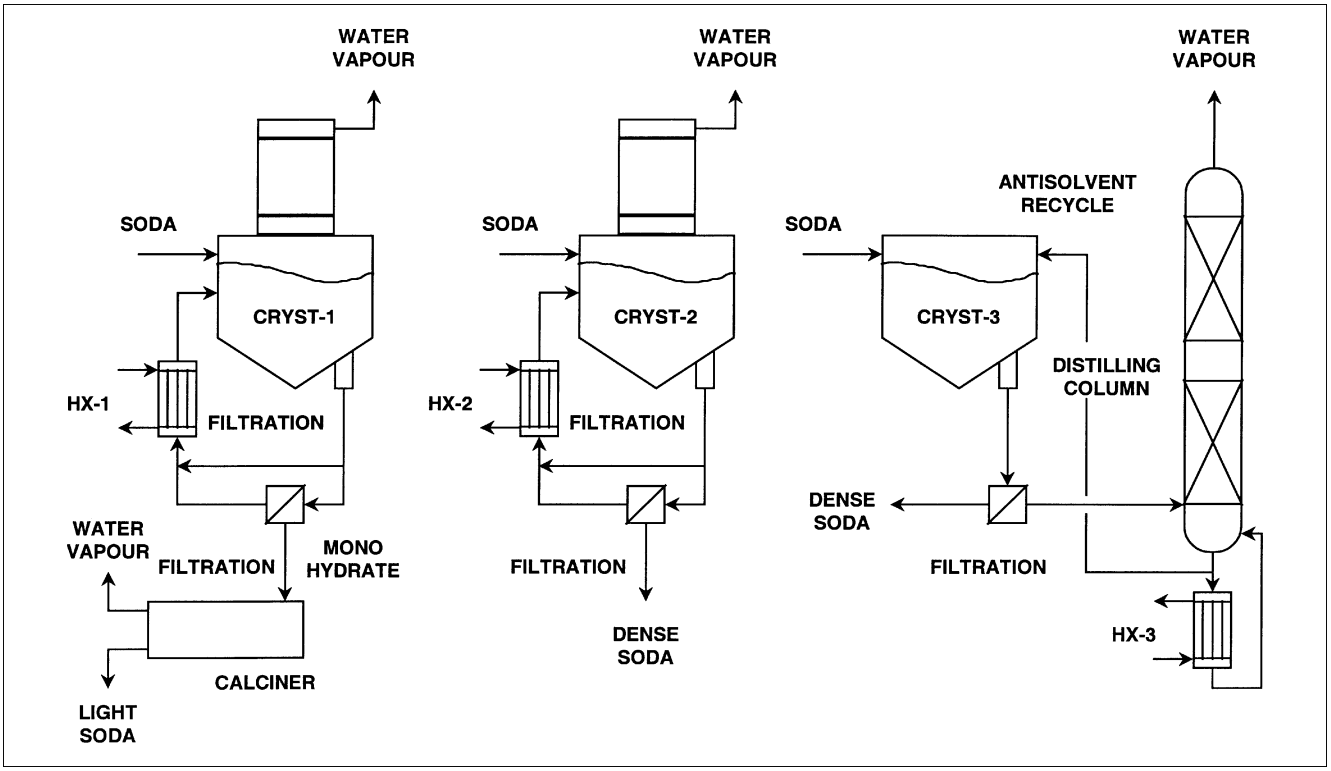

Figure 1. Production of anhydrous sodium carbonate.

Conventional crystallization and subsequent calcining of monohydrate (left), evaporative crystallization from mixed solvent (middle), and direct crystallization with antisolvent (right; regeneration of the antisolvent by means of distillation).

same time little (anti)solvent evaporates. The present work does not focus on this option; a more detailed description is given by Meijer et al. (1998).

In this work, the third option (Figure 1, right) is studied: during antisolvent crystallization, the antisolvent is mixed with the solvent (in this case, water), in which the solute (Na_2CO_3) is dissolved. Because the antisolvent interacts strongly with the solvent, mostly because of hydrogen bonding, the solubility of the solute is decreased and soda is forced to crystallize. Successful application of this option depends strongly on the phase behavior of the antisolvent used: the antisolvent has to reduce both the solubility and the water activity, but it is also necessary that it has a high boiling point, because the crystallization will probably be carried out at temperatures of about 80° to 100°C. This means that the more common antisolvents like ethanol and acetone cannot be used because of their low boiling points (78 and 56°C, respectively). Finally, regeneration has to be energy-friendly.

The antisolvents used in this work are ethylene glycol (EG; boiling point of 198°C) and diethyleneglycol (DEG; boiling point of 244°C), because these antisolvents were found to be fully miscible with saturated sodium carbonate solutions (Oosterhof et al., 1999).

Two simple models are proposed, describing the relation between the water activity and the transition temperature. Water activities are calculated at different temperatures and mixture compositions from measured vapor pressures. Finally, continuous crystallization experiments are carried out using both DEG and EG as antisolvent, in order to validate the predictions of the model and to investigate the quality of the crystal product.

Theory

Two methods are introduced in this section to describe the influence of the water activity on the transition point at which sodium carbonate anhydrate and monohydrate are in equilibrium. The first method uses the thermodynamic solubility product of both hydrates, while the second method treats the transition between the hydrates as an equilibrium reaction.

Solubility products

The chemical potential of sodium carbonate anhydrate (AH) in solution is given by

$$\mu_{AH,L} = \mu^0 + RT \cdot \ln\left[(\mathrm{Na}^+)^2 \cdot (\mathrm{CO}_3^{2-})\right], \qquad (1)$$

where (Na^+) and (CO_3^{2-}) represent the activities of the components in solution, and μ^0 is the chemical potential of (hypothetical) liquid Na_2CO_3 under standard conditions (298.15 K, 1 bar, and all activities equal to 1). At the solubility concentration of AH, the chemical potentials of the liquid and the solid phase are equal:

$$\mu_{AH,S} = \mu_{AH,L} \quad \text{(at solubility concentration of AH)}. \qquad (2)$$

The value of ($\mu_{AH,S} - \mu^0$), which is derived by substitution of Eq. 2 into Eq. 1, follows from the thermodynamic solubility product, K_{SP}^{AH}

$$\mu_{AH,S} - \mu^0 = RT \cdot \ln\left(K_{SP}^{AH}\right) = RT \cdot \ln\left[(\mathrm{Na}^+)^2 \cdot \left(\mathrm{CO}_3^{2-}\right)\right]. \tag{3}$$

Similar relations can be derived for sodium carbonate monohydrate (MH):

$$\mu_{MH,S} = \mu_{MH,L} \quad \text{(at solubility concentration of MH)} \tag{4}$$

$$\mu_{MH,S} - \mu^0 = RT \cdot \ln\left(K_{SP}^{MH}\right) = RT \cdot \ln\left[(\mathrm{Na}^+)^2 \cdot \left(\mathrm{CO}_3^{2-}\right) \cdot (\mathrm{H_2O})\right]. \tag{5}$$

Both thermodynamic solubility products can be calculated from stable and metastable solubility data. For anhydrate:

$$K_{SP}^{AH} = (\mathrm{Na}^+)_{\mathrm{eq}}^2 \cdot \left(\mathrm{CO}_3^{2-}\right)_{\mathrm{eq}} = \gamma_{\mathrm{Na}^+}^2 \cdot [\mathrm{Na}^+]_{\mathrm{eq}}^2 \cdot \gamma_{\mathrm{CO}_3^{2-}} \left[\mathrm{CO}_3^{2-}\right]_{\mathrm{eq}}; \tag{6}$$

and for monohydrate:

$$K_{SP}^{MH} = (\mathrm{Na}^+)_{\mathrm{eq}}^2 \cdot \left(\mathrm{CO}_3^{2-}\right)_{\mathrm{eq}} \cdot (\mathrm{H_2O}) = \gamma_{\mathrm{Na}^+}^2 \cdot [\mathrm{Na}^+]_{\mathrm{eq}}^2 \cdot \gamma_{\mathrm{CO}_3^{2-}} \left[\mathrm{CO}_3^{2-}\right]_{\mathrm{eq}} \cdot \gamma_{\mathrm{H_2O}} \cdot [\mathrm{H_2O}]. \tag{7}$$

The subscript *eq* refers to the solubility concentration, and the activity coefficients are calculated using the method proposed by Pitzer (Peiper and Pitzer, 1982; Pitzer, 1991). The coefficients that were used for the calculations are: $\beta^{(0)} = 0.0362$, $\beta^{(1)} = 1.51$, and $C^{\phi} = 0.0052$. The equations used to calculate the activity coefficients are given in the Appendix.

The transition point can now be calculated using

$$\mu_{\mathrm{H_2O}} + \mu_{AH,S} = \mu_{MH,S} \quad \text{(at the transition point)}. \tag{8}$$

When Eqs. 3 and 5 are inserted into Eq. 8 for both MH and AH, one can derive

$$a_W^{TR}(T) = \frac{K_{SP}^{MH}(T)}{K_{SP}^{AH}(T)} = (\mathrm{H_2O}) \quad \text{(at the transition point)}. \tag{9}$$

When both solubility products are inserted in Eq. 9, the water activity at which the anhydrous and the monohydrous phase are in equilibrium can be calculated as a function of the temperature. This so-called transition curve is given in Figure 2.

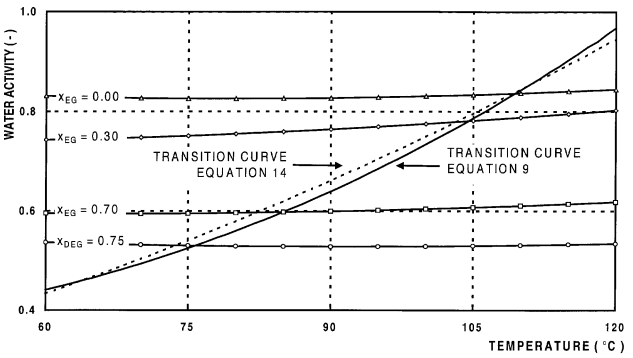

Figure 2. Two calculated transition curves according to Eqs. 9 and 14 and some measured water activities in ternary mixtures.

The transition temperature can easily be deduced from this figure for mixtures containing various types and concentrations of antisolvent.

Equilibrium reaction

Another way to describe the influence of the water activity on the transition temperature is by treating the recrystallization step as an equilibrium reaction. Consider the following reaction:

$$\mathrm{Na_2CO_3} + \mathrm{H_2O} \Leftrightarrow \mathrm{Na_2CO_3 \cdot 1H_2O} + Q_{0\to 1}, \tag{10}$$

in which $Q_{0\to 1}$ is the heat produced during the transition (J/mol). Assuming that no mechanical work is done by the system and that pressure and temperature remain constant, the reaction enthalpy equals the heat produced:

$$Q_{0\to 1} = \Delta H_{r,0\to 1}. \tag{11}$$

The equilibrium constant for the recrystallization reaction is given as

$$K_{0\to 1} = \frac{1}{a_W}, \tag{12}$$

in which a_W again is the water activity of the mixture. The influence of temperature on the value of equilibrium constant $K_{0\to 1}$ can be described with:

$$\frac{\partial \ln K_{0\to 1}}{\partial T} = \frac{\Delta H_{r,0\to 1}}{R \cdot T^2}. \tag{13}$$

Integration of Eq. 13 subsequently gives

$$a_W^{TR}(T) = a_W^{TR}(T_{\mathrm{ref}}) \cdot \exp\left[-\frac{\Delta H_{r,0\to 1}}{R} \cdot \left(\frac{1}{T} - \frac{1}{T_{\mathrm{ref}}}\right)\right], \tag{14}$$

where $a_W(T_{\mathrm{ref}})$ is the water activity at reference temperature T_{ref}. It is logical to choose the transition temperature in pure soda solutions as the reference temperature: at 109°C, the water activity is 0.835 (Freier, 1978). Assuming $\Delta H_{r,0\to 1}$ to be independent of temperature, the recrystallization temperature can now be calculated at a given temperature.

The value of $\Delta H_{r,0\rightarrow 1}$ was taken to be 14.2 kJ/mol (Du Maire, 1928). The transition curve based on this approach also is given in Figure 2. As can be seen from this figure, the two routines, which both use binary data only, give almost the same prediction for the influence of the amount and type of antisolvent on the location of the transition temperature.

Water activity measurement

Calculation of the water activity in a ternary system is rather complicated, but its measurement is relatively easy when water is the only component in the system that has a substantial vapor pressure at the temperature of interest. This means that if the vapor above the mixture is presumed to behave ideally, the water activity can be calculated from

$$a_W(T) = \frac{p(T)}{p^0_{\text{water}}(T)}, \tag{15}$$

where a_W is the water activity, p is the measured vapor pressure, and p^0_{water} is the vapor pressure over pure water, all at temperature T. In Eq. 15, the vapor pressures of sodium carbonate and the antisolvent (AS) are assumed to be negligible, so

$$p(T) = \gamma_{\text{water}} \cdot x_{\text{water}} \cdot p^0_{\text{water}} + \gamma_{\text{soda}} \cdot x_{\text{soda}} \cdot p^0_{\text{soda}} + \gamma_{AS} . x_{AS} \cdot p^0_{AS} \approx \gamma_{\text{water}} \cdot x_{\text{water}} \cdot p^0_{\text{water}} \equiv a_W \cdot p^0_{\text{water}}, \tag{16}$$

in which x_i is the mol fraction and γ_i the activity coefficient of component i (with i water, soda, or AS).

Experimental Studies

Two types of experiments were carried out. First, vapor pressures were measured above mixtures of water and EG (or DEG), saturated with sodium carbonate; and secondly, continuous crystallization experiments were carried out using EG and DEG as antisolvents.

Double-distilled water, ethylene glycol (Merck, $>99\%$), diethyleneglycol (Aldrich, $>99\%$), and sodium carbonate (Akzo Nobel, purity at least 99%) were used throughout all experiments.

Vapor pressures

All measurements were carried out in a 1-L jacketed thermostated vessel, which was heated with a Lauda-type thermostat equipped with external temperature control. The temperature in the vessel was measured with an accuracy of 0.05°C. The vapor pressure above the mixtures was recorded with a Druck PTX-610 pressure transmitter (accuracy 5 mBar). At the start of each experiment, the vessel was charged with approximately 500 g of the sample and a sufficient amount of sodium carbonate to ensure saturation at all temperatures. The vessel was subsequently closed and a vacuum pump was used to decrease the pressure over the sample. The temperature of the system was kept at a fixed value for a period of 3 h, so that chemical equilibrium could be reached (this was found to be sufficiently long). The temperature was increased in steps of 5°C from 60°C to 120°C.

Table 1. Experimental Information for the Crystallization Experiments Carried Out at Weight-Fraction Antisolvent $x_{AS} = (m_{AS} + m_{water})$ in the Crystallizing Mixture, and at temperature T

x_{AS}	T (°C)	c^* (wt. % Na_2CO_3)	ζ (%)	M_T (wt. %)
Ethylene Glycol				
0.50	80	9.1	9	0.9
0.60	60	7.2	12	0.9
0.60	80	6.8	17	1.4
0.70	95	5.3	15	0.9
0.80	90	4.0	5	0.2
Diethyleneglycol				
0.67	80	0.8	89	6.1
0.67	90	1.7	76	5.2
0.67	100	1.7	76	5.2
0.75	75	0.7	87	4.5
0.75	80	0.3	95	4.9
0.75	85	0.7	87	4.5
0.75	90	1.0	82	4.2
0.80	70	0.7	84	3.5
0.80	80	0.2	95	4.0
0.80	85	0.5	89	3.7

Soda solubility c^* (from Oosterhof et al., 1999) at prevailing conditions. Calculated theoretical soda recovery, ζ and weight percentage crystals in the crystallizer, M_T.

Continuous crystallization experiments

The continuous crystallization experiments were carried out in a 1-L jacketed glass crystallizer, equipped with four baffles and a 50-mm turbine stirrer. Two Watson Marlow peristaltic pumps were used to add the antisolvent and the brine (18 wt. % sodium carbonate) to the crystallizer and a Lauda thermostat provided heating (accuracy 0.1°C). The slurry was removed continuously from the reactor via an outlet overflow. To determine whether the crystals were hydrated or not, a sample was taken from the outlet of the reactor every 30 min. The product was filtered, washed with ethanol, weighed, and dried in an oven: first for 1 h at 50°C to remove the ethanol, then at 150°C for at least 24 h to evaporate all crystal water, if present. Furthermore, the crystals were observed with a light microscope and a scanning electron microscope (SEM) in order to study the morphology. The bulk density of the crystal product was also determined by weighing a measured volume of particles. The most important information about the continuous crystallization experiments is given in Table 1. The solubilities were taken from earlier work (Oosterhof et al., 1999).

Soda solubility c^* at the prevailing temperature and antisolvent-to-water ratio in the crystallizer are given together with salt recovery, ζ, and weight percentage of crystals in the crystallizer, M_T. Salt recovery ζ is calculated using

$$\zeta = 1 - c^*/c^\circ, \tag{17}$$

with c^* the solubility concentration of the salt and c° the salt concentration of the brine feed, both concentrations expressed in gram salt per 100 g water. The theoretical weight-percentage crystals in the crystallizer, M_T, is calculated from a mass balance on the crystallizer. The particle-size distribution of the product was measured using a Coulter Multisizer II.

Table 2. Fitted Values of a and b in Eq. 18 for Various Mixtures with Weight Fraction Antisolvent, x_{AS}

x_{EG}	a	b (K)	x_{DEG}	a	b (K)
	Ethylene Glycol			Diethyleneglycol	
0.00	20.25	−5048	0.00	20.25	−5048
0.10	20.30	−5073	0.50	20.31	−5087
0.20	20.44	−5134	0.67	20.18	−5081
0.30	20.54	−5182	0.75	20.06	−5096
0.40	20.39	−5139	0.80	19.41	−4897
0.50	20.48	−5201			
0.67	20.27	−5183			
0.70	19.68	−5004			
0.75	19.48	−4952			
0.80	19.30	−4931			

Note: The correlation coefficient for the Clausius−Clapeyron equations was at least 0.99 in all cases.

Results and Discussion

Vapor pressure measurements

The experimental data were correlated using the Clausius-Clapeyrons equation:

$$\ln(p) = a + \frac{b}{T}. \tag{18}$$

The fitted values for a and b are given in Table 2 for the various mixtures with EG or DEG. The water activity in the various mixtures was calculated using Eq. 15. Some of the measured water activities are given as a function of temperature in Figure 2. The transition curves of Eqs. 9 and 14 are also given. The influence of the antisolvent is obvious: when the fraction antisolvent in the mixture increases, the water activity decreases. The water activity is only weakly influenced by temperature. The temperature at which each curve intersects with the transition line is the transition temperature of Na_2CO_3 (MH to AH) in the mixture of interest.

The various transition points are plotted in Figure 3 as a function of the weight-fraction antisolvent in the mixture,

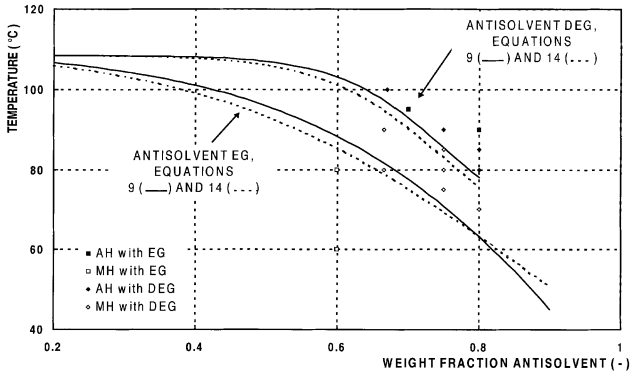

Figure 3. Transition temperature plotted as a function of the weight-fraction antisolvent in the mixture for both ethylene glycol and diethyleneglycol.

The markers represent continuous crystallization experiments. Solid markers are for anhydrate; open markers are for monohydrate. DEG is depicted with a diamond; EG with a square.

Table 3. Predicted Transition Temperatures (According to Eqs. 9 and 14), Observed Hydrate and Measured Anhydrate Bulk Density, and Average Volume-Based Particle Size (m_4/m_3) for Crystallization Experiments Carried Out at dWeight-Fraction Antisolvent, x_{AS}, and Temperature T

	T	*Predicted* T_{TR}		*Observed*	ρ_{bulk}	m_4/m_3
x_{EG}	(°C)	Eq. 9	Eq. 14	*Hydrate*	(kg/m^3)	(μm)
Ethylene Glycol						
0.50	80	93.9	96.4	MH	—	—
0.60	60	86.2	89.1	MH	—	—
0.60	80	86.2	89.1	MH	—	—
0.70	95	76.3	78.8	AH	940	—
0.80	90	64.6	64.8	AH	890	—
Diethyleneglycol						
0.67	80	95.4	97.9	MH	—	—
0.67	90	95.4	97.9	MH	—	—
0.67	100	95.4	97.9	AH	900	207
0.75	75	83.1	85.5	MH	—	—
0.75	80	83.1	85.5	MH	—	—
0.75	85	83.1	85.5	MH	—	—
0.75	90	83.1	85.5	AH	920	164
0.80	70	75.8	78.1	MH	—	—
0.80	80	75.8	78.1	AH	800	123
0.80	85	75.8	78.1	AH	850	125

both for EG and DEG. The solid lines are based on Eq. 9, while the slightly different dashed lines represent the points of intersection with the equilibrium curve of Eq. 14. From this graph, the minimum temperature at which anhydrous soda is stable can be determined for each weight-fraction antisolvent in the crystallizing mixture. When comparing mixtures with the same weight-fraction antisolvent, EG is found to have a stronger effect on the transition temperature than DEG.

Continuous crystallization experiments

Hydrate Stability. The results of the vapor pressure measurements were used to determine the transition temperature for each crystallizing mixture: both values of T_{TR} (based on Eqs. 9 and 14) are given in Table 2: if $T > T_{TR}$, anhydrate is expected; if $T < T_{TR}$, monohydrate is expected. In Figure 3 and Table 3 the predictions are compared with the results of the continuous experiments. Table 3 also lists the temperatures and the antisolvent fractions as well as the stable hydrate form and some product features.

Considering the fact that both transition curves are based on binary data only, the accuracy and the predictive value are very good. Only one deviation is recorded for the transition curve based on the solubility products (Eq. 9). Thus, the models are very well able to predict the transition temperature.

Product Features. The difference between monohydrate and anhydrate crystals is distinct: this is shown in Figure 4 and Figure 5. In the first picture, long needle-shaped crystals are visible, and in the second, round anhydrate crystals can be seen, produced at the same experimental conditions as the monohydrate but at a slightly higher temperature. The anhydrous soda consists of multiple-faceted crystalline particles that do not seem to be true agglomerates.

There is no distinct influence of the operating conditions in the crystallizer on the bulk density of the product: it varies

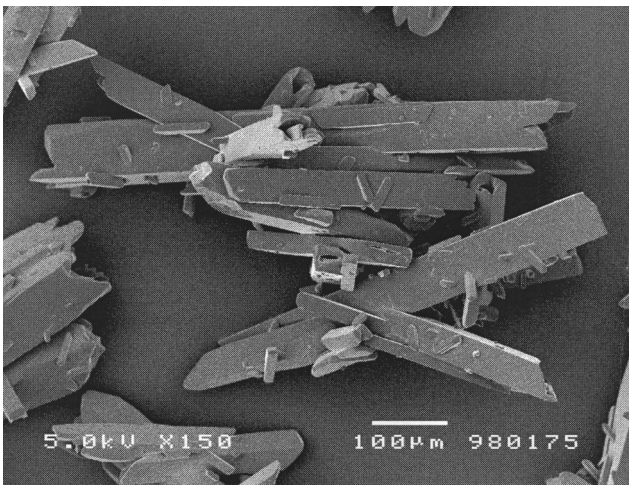

Figure 4. Monohydrous sodium carbonate, crystallized with ethylene glycol, $x_{EG} = 0.67$ at 90°C.

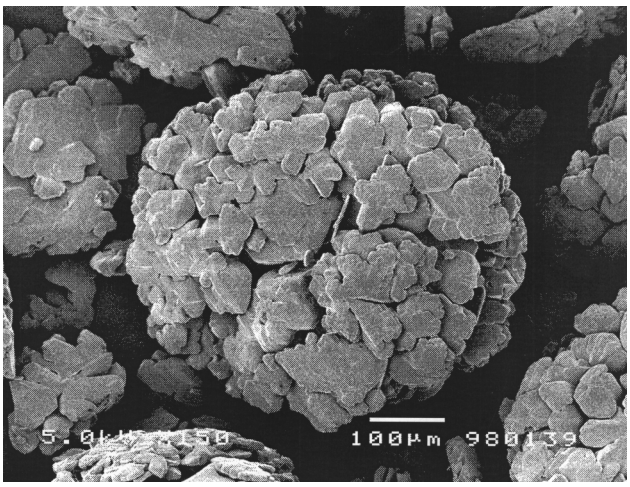

Figure 5. Anhydrous sodium carbonate, crystallized with ethylene glycol, $x_{EG} = 0.67$ at 100°C.

between 800 and 950 kg/m^3, which is significantly higher than that of conventionally produced light soda. It seems that the bulk density is not strongly influenced by the type of the antisolvent. Finally, some average particle sizes of the anhydrous product are given in Table 3, only for the crystals produced with DEG. When EG was used as the antisolvent, the product was too coarse to analyze it with the Coulter Multisizer. An increased weight fraction of DEG in the mixture decreases the average particle size of the product from 207 μm to 123 μm. This is probably due to the fact that a large weight fraction DEG results in a low soda solubility and thus a high supersaturation in the crystallizer. Visual observation of the product from EG showed the same trend. Dominant crystal sizes were larger: around 500 μm, which is due to the milder conditions, that is, a lower supersaturation in the crystallizer, and thus less nucleation.

Conclusions

The water activity at which sodium carbonate anhydrate and monohydrate are in equilibrium can be calculated from binary (water/soda) data only. By determining the water activity from vapor-pressure measurements in ternary mixtures, the transition temperatures above which anhydrate is stable can be predicted. The model using thermodynamic solubility products from binary mixtures yielded about the same prediction as the model using the equilibrium reaction. Both predictions are almost as good, as follows from the comparison with the results of continuous crystallization experiments.

Bulk densities for anhydrate of up to almost 1,000 kg/m^3 are obtained, while the particle size decreases with increasing amounts of antisolvent in the mixture, both for EG and DEG. Anhydrate produced with EG had significantly larger average particle sizes than that crystallized with DEG. Comparison of all experiments at which AH was crystallized showed that the average particle size increased uniformly with the solubility of the soda in the crystallizing mixture.

Literature Cited

Du Maire, M., *Gmelins Handbuch der Anorganische Chemie - Natrium*, Chemie Verlag, Berlin, p. 730 (1928).

Fleischmann, W. G., "Untersuchungen zur Verdrängungskristallisation von Natriumsuflat aus Wässeriger Lösung mit Methanol," PhD Diss., Univ. of München, München, Germany (1984).

Freier, R. K., *Aqueous Solutions. Data for Inorganic and Organic Compounds*, Vol. 2, Supplements, Gruyter, Berlin, p. 333 (1978).

Meijer, J. A. M., R. M. Geertman, H. Oosterhof, and G. J. Witkamp, "Production of Water-Free Soda," European Patent, No. 9720481.0-1218.

Oosterhof, H., G. J. Witkamp, and G. M. van Rosmalen, "Some Antisolvents for Crystallisation of Sodium Carbonate," *J. Fluid Phase Equilibria*, **155**(2), 229 (1999).

Peiper, J. C., and K. S. Pitzer, "Thermodynamics of Aqueous Carbonate Solutions Including Mixtures of Sodium Carbonate, Bicarbonate, and Chloride," *J. Chem. Thermodyn.*, **14**, 613 (1987).

Pitzer, K. S., *Activity Coefficients in Electrolyte Solutions*, 2nd ed., CRC Press, Boca Raton, FL (1991).

Weingärtner, D. A., S. Lynn, and D. N. Hanson, "Extractive Crystallization of Salts from Concentrated Aqueous Solution," *Ind. Eng. Chem. Res.*, **30**, 490 (1991).

Appendix: Pitzer Equations

Pitzer's equations (Pitzer, 1991) are a very useful and adequate method for calculating activity coefficients of water and ions in (mixtures of) electrolyte solutions. This Appendix contains the equations that are needed to calculate these activity coefficients. Little attention is given to the physical meaning of the various equations; more fundamental information can be found in Peiper and Pitzer (1982) and Pitzer, (1991).

An electrolyte MX that consists of ν_M anions with charge z_M, and ν_X cations with charge z_X is dissolved in water and has a molal concentration of m moles per kilogram water. The ionic strength of that solution is given by

$$I = \frac{1}{2} \cdot \sum_i m_i \cdot z_i^2 = \frac{1}{2} \cdot \left(m_M \cdot z_M^2 + m_X \cdot | z_X^2 | \right), \quad \text{(A1)}$$

in which m_M and m_X are the molal concentrations of the anion and the cation:

$$m_M = \nu_M \cdot m$$
$$m_X = \nu_X \cdot m. \quad \text{(A2)}$$

The activity coefficients of ions M and X, the osmotic coefficient ϕ, and the water activity are now calculated using:

$$\ln \gamma_M = z_M^2 \cdot F + \sum_a m_a \cdot (2 \cdot B_{Ma} + Z \cdot C_{Ma}) + z_M \cdot \sum_c \sum_a m_c \cdot m_a \cdot C_{ca} \quad \text{(A3)}$$

$$\ln \gamma_X = z_X^2 \cdot F + \sum_c m_c \cdot (2 \cdot B_{cX} + Z \cdot C_{cX}) + |z_X| \cdot \sum_c \sum_a m_c \cdot m_a \cdot C_{ca} \quad \text{(A4)}$$

$$\phi = 1 + \frac{2}{\sum_i m_i} \cdot \left(\frac{-A_\phi \cdot I^{3/2}}{1 + b \cdot I} + \sum_c \sum_a m_c \cdot m_a \cdot \left(B_{ca}^\phi + Z \cdot C_{ca} \right) \right), \quad \text{(A5)}$$

in which we define:

$$Z = \sum_i m_i \cdot |z_i|. \quad \text{(A6)}$$

The Debije-Hückel parameter, A_ϕ:

$$A_\phi = \frac{1}{3} \cdot \sqrt{\frac{2\pi N_0 d_w}{1{,}000}} \cdot \left(\frac{e^2}{\epsilon k T} \right)^{3/2} \quad \text{(A7)}$$

and some other parameters (not mentioned by name):

$$F = -A_\phi \cdot \left(\frac{\sqrt{I}}{1 + b \cdot \sqrt{I}} + \frac{2}{b} \cdot \ln\left(1 + b \cdot \sqrt{I}\right) \right) + \sum_c \sum_a m_c \cdot m_a \cdot B'_{ca} \quad \text{(A8)}$$

$$B_{MX}^\phi = \beta_{MX}^0 + \beta_{MX}^1 \cdot \exp\left(-\alpha_1 \cdot \sqrt{I}\right) + \beta_{MX}^2 \cdot \exp\left(-\alpha_2 \cdot \sqrt{I}\right) \quad \text{(A9)}$$

$$B_{MX} = \beta_{MX}^0 + \beta_{MX}^1 \cdot g\left(-\alpha_1 \cdot \sqrt{I}\right) + \beta_{MX}^2 \cdot g\left(-\alpha_2 \cdot \sqrt{I}\right) \quad \text{(A10)}$$

$$B'_{MX} = \frac{\beta_{MX}^1 \cdot g'\left(-\alpha_1 \cdot \sqrt{I}\right) + \beta_{MX}^2 \cdot g'\left(-\alpha_2 \cdot \sqrt{I}\right)}{I}. \quad \text{(A11)}$$

From Eq. 23 the water activity, a_W, is calculated:

$$a_W = \exp\left(-\phi \cdot \frac{\sum_i m_i}{55.6} \right). \quad \text{(A12)}$$

Subscripts a and c denote other anions and cations that are present in the solution. Only the second virial coefficient was used in the deduction and no terms for asymmetrical mixing were used.

In Eqs. 27 to 29, the constants α_1, α_2, β^1, and β^2 are introduced. For 2-2 salts $\alpha_1 = 1.4$ and $\alpha_2 = 12.0$, for other salts $\alpha_1 = 2.0$ and $\alpha_2 = 0$. The appropriate values for β^0, β^1, and β^2 and their dependency of temperature can be found in the literature (Peipes and Pitzer, 1982). For clarity, the functions $g(x)$ and $g'(x)$ were inserted in Eqs. 28 to 29:

$$g(x) = \frac{2 \cdot [1 - (1 + x) \cdot \exp(-x)]}{x^2} \quad \text{(A13)}$$

$$g'(x) = -\frac{2 \cdot \left[1 - \left(1 + x + \frac{x^2}{2} \right) \cdot \exp(-x) \right]}{x^2}. \quad \text{(A14)}$$

The Pitzer coefficients for sodium carbonate solutions given in the literature are:

$$\beta^0 = 1.79 \times 10^{-3} \cdot (T - 298.15) + 0.0362$$

$$\beta^1 = 2.05 \times 10^{-3} \cdot (T - 298.15) + 1.51$$

$$C = 0.0052, \quad \text{(A15)}$$

with T the temperature in Kelvin.

After comparison of the simulated results with experimental data from the literature, however, the temperature-dependent terms of β^0 and β^1 were omitted.

Manuscript received Sept. 7, 1999, and revision received July 17, 2000.